

Prediction of EDM Process Parameters for AISI 1020 Steel using RSM, GRA and ANN

R. Rajesh, M. Dev Anand

Abstract--- AISI 1020 Steel is hard while machining because of its nature of harness and brittleness. Electrical Discharge Machining (EDM) is a significant technique to machine such materials. Current research examines the pulse current effect (A), discharge voltage (B), pulse on time (C), pulse off time (D), Oil pressure (E) and spark gap (F) on Metal Removal Rate (MRR) and Surface Roughness on EDM of AISI 1020 Steel. Experiments have been carried out in a methodical type taking up nearly 54 successive trails utilizing an EDM machine and a copper electrode of 10mm diameter. Three factors, three levels, Box Behken through response surface methodology design was utilized to analyze the outcomes. Gray relational analysis techniques are adopted for finding parameter influencing range for MRR and SR. A multi regression mathematical model was brought up in launching the association between parameters of machining and artificial neural network techniques are used for predicting the optimized parameters.

Keywords--- Electro Discharge Machining, Response Surface Methodology, Gray Relational Analysis, Artificial Neural Network, Material Removal Rate, Surface Roughness.

I. INTRODUCTION

With the advancement of scientific technology, incorporation of products to aid multi-functional purposes turn out to be the tradition. Product size reduction is consequently extremely necessary. Attaining this impartial could have need of fresh hard materials with greater strength and temperature-resistance. Though, with the exclusion of drilling, traditional machining techniques are not relevant to these novel materials. Hence, it is essential to cultivate innovative machining process. EDM utilizes high frequency pulse discharge within the electrode and the work piece for producing the vaporization phenomenon and melting at the electric discharge point. At that point itself, heating of dielectric occurs instantly to an enormously high temperature so that the work piece material's small portion is raised up above its melting point and consequently that has been carried away. In EDM, the tool electrode never get in touch with the work piece, and is practically non loaded. The process functions very proficiently for AISI 1020 steel machining.

Dissimilar researchers have performed optimization of process parameter of dissimilar types of EDM from time to time involving is similar optimization models and solution techniques. Reviews of those past studies have variable bounds, objective functions, constraints, prominent decision variables, remarks and their limitation. The results were recapitulated as follows: KuldeepOjha et al., (2010), inform research on EDM relating to enhancement in MRR along

with few insight into material removal mechanism. Tolga Bozdana et al.(2010), report that experimental investigation of EDM drilling of Ø2mm holes on Inconel718 using brass electrode. The effect of process parameters on process outputs was reported based on minimum number of experiments. The mathematical modeling of process has been performed using Response Surface Methodology (RSM). The results show that the developed model can attain reliable prediction of experimental results within acceptable accuracy. MusraatAli et al., (2009), Differential Evolution (DE) is an influential yet simple Evolutionary Algorithm (EA) to optimize real valued, multimodal functions. B.H. Yan, et al., (1999), reviews the characteristics of micro hole and minimal tool electrode wear rate in obtaining a high precision micro-hole in the carbide, the polarity changing effects, the shape and the rotational speed of tool electrode tool electrode are premeditated. S. S. Mahapatra, et al., (2006), proposed to research factors like pulse duration, discharge current, wire speed, pulse frequency, wire tension and dielectric flow rate and few preferred communications both for MRR maximizations and SR minimization in WEDM process involving Taguchi method. Qing GAO et al., (2008), depicts Artificial Neural Network (ANN) and Genetic Algorithm (GA) are exclusively utilized in creating the parameter optimization model. An ANN model that adapts L-M algorithm was set up to depict the association among MRR and input parameters, and GA is utilized in optimizing parameters to obtain results. The model exhibited is much efficient, and MRR is progressed using machining parameters that were optimized. M. R. Shabgard, et al., (2009), endeavor was involved in developing mathematical models to relate the MRR, TWR (Tool Wear Rate) and SR to machining parameters. Moreover, a study was performed in analyzing the machining parameters effects in respect of itemized technological characteristics. SushantDhar, et al., (2007), describes Aluminium matrix composites are hard while machining because of the occurrence of hard and brittle ceramic reinforcements. EDM is a significant process to machine such materials. The work estimates the effect of Current (c), Pulse-On Time (p) and air Gap Voltage (v) on MRR, TWR, and Radial Over Cut (ROC) on EDM of Al-4Cu-6Si alloy-10% weightSiC_p composites. Conditions favouring for maximum MRR with condensed TWR and ROC can also be achieved through linear programming. The MRR, TWR and ROC goes up considerably in a nonlinear manner with enhanced current. Puertaset al., (2003), this work is concentrated on features associated to surface quality and dimensional precision, that seems to be the highly predominant parameters form the point of view of

Revised Manuscript Received on July 10, 2019.

R. Rajesh, Associate Professor, Department of Mechanical Engineering, Noorul Islam Centre for Higher Education, Kumaracoil, Tamil Nadu, India.

M. Dev Anand, Professor and Deputy Director, Academic Affairs, Department of Mechanical Engineering, Noorul Islam Centre for Higher Education, Kumaracoil, Tamil Nadu, India.
(e-mail: anandpmt@hotmail.com)

choosing not only the processes optimum conditions but also the inexpensive aspects. Thillaivanan, et al., (2010), suggested practical method to optimize cutting parameters for EDM under the least total machining time supported by Taguchi Method and ANN is accessible. Provided methodology is not only economical and less time consuming but effective and accurate in examining the parameters of machining. Current has been identified to be a noteworthy control on the total time of machining. As an outcomes, the performance attributes like total machining time could be made better through this technique. Sameh S. H(2009)shows the improvement of a wide-ranging mathematical model to correlate the communicating and higher order manipulation of numerous EDM parameters through RSM, utilizes appropriate experimental data as acquired via conducting tests. The mathematical models was brought up on the basis of RSM, employing the data from practical noticeable settings of the EDM of work pieces. Exploration was performed to analyze the control circumstances demanded in controlling MRR, Electrode Wear Ratio (EWR), gap size and SR. Seung-Han Yang et al., (2009), recommends a methodology to optimize for the choice of finest process parameters of EDM. Regular cutting experiments have been performed on die-sinking machine under dissimilar conditions of process parameters. This system model is utilized to instantaneously maximize the MRR together with minimize the SR involving SA scheme. Ramezan Ali MahdaviNejad(2011),proposed the work

which aims the optimization of SR and MRR of EDM of SiC_p parameters concurrently. As the output parameters are contradictory naturally, hence there exists no single association of machining parameters, making available with the idle machining performance. ANN with back propagation algorithm has been utilized to reproduce the process. A multi-objective optimization method, non dominating sorting genetic algorithm-II has been utilized in optimizing the process. Three significant process input parameters effect viz., discharge current, pulse on time (Ton), pulse off time (T_{off}) on EDM of SiC are believed. Experiments were performed over a collection of deliberated input parameters for training and verification of the model. G. Krishna MohanaRao et al., (2010),work is intended in surface hardness optimization formed in die dipping EDM by preferring the instantaneous effect of various input parameters. The experiments are performed on Ti6Al4V, HE15, 15CDV6 and M-250 by modifying the peak current and voltage and the associated hardness values were measured. Majumder, et al., (2012),propose investigation of the process parameters of EDM has optimized for minimum EWR. The machining parameters used in this study are spark-current, pulse-on duration and pulse-off duration. The relation between electrode wear rate and machining parameters has been developed by using RSM. The main reason of this work is to demonstrate the input process distinctiveness of EDM and has influenced by the process parameters.

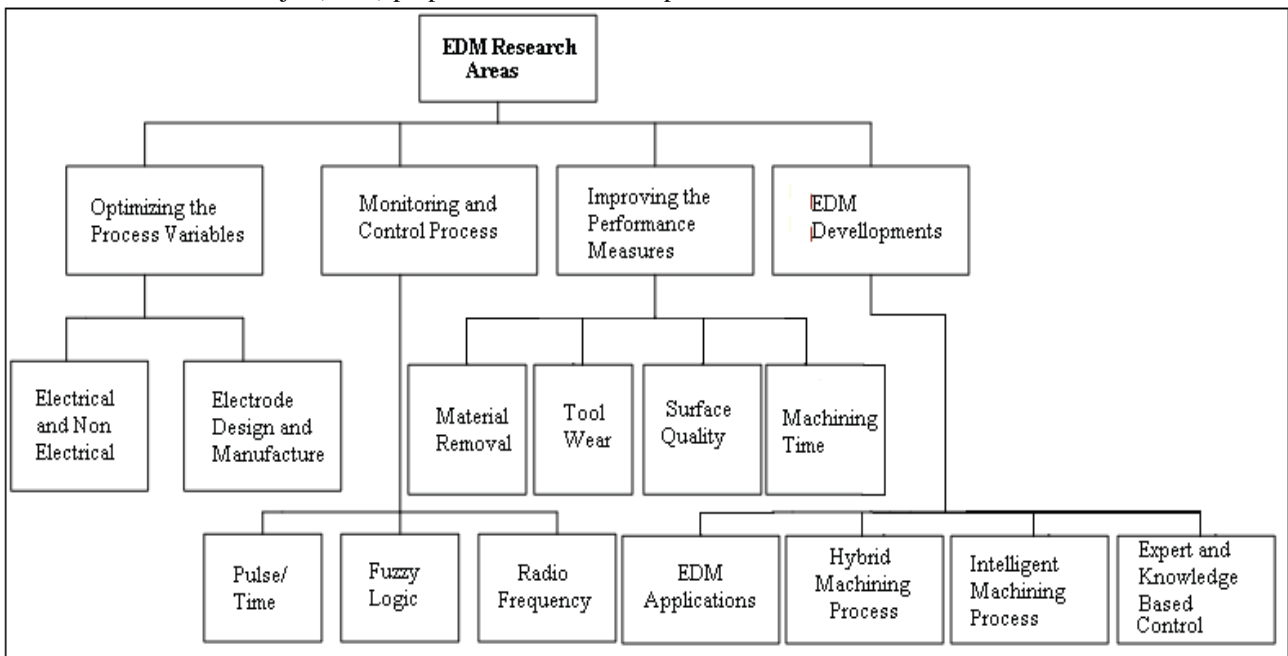


Figure 1: Classification of Major EDM Research Areas

These works demonstrate a study of the intervening variable in EDM of material AISI 1020 Steel, the MRR and SR were studied. Six more influential parameters were used during the experiments. The result illustrate that current was the predominant parameter influencing the MRR. Different investigators were presents the cataloging of the numerous research areas in EDM and probable future research directions as illustrated in Figure 1. The retro analysis of literature exposed and brought out into view that no works were performed in EDM of AISI 1020 steel and with more than three parameters.

II. EDM MACHINE

With Electronica 5030 Die Sinking EDM machine experiments were conducted as shown in Figure 2. The dielectric fluid and electrode flushing method was utilized.



Figure 2: Electronica 5030 Die Sinking EDM Machine

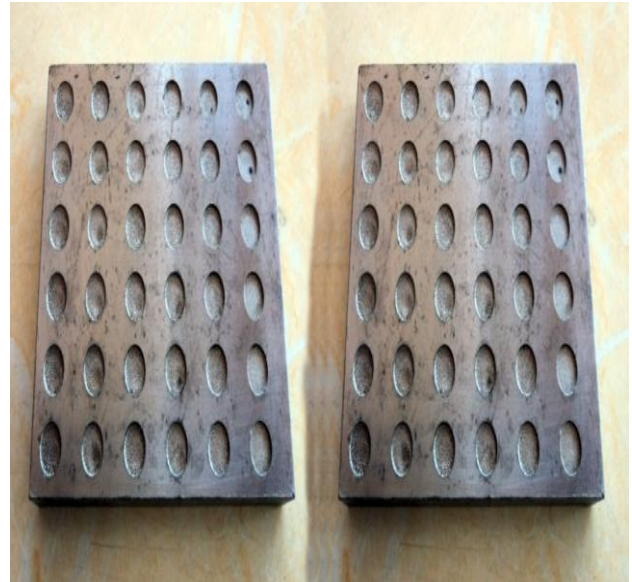


Figure 3: Electronica 5030 Die Sinking EDM Machining Process Underway

III. EXPERIMENTAL PROCEDURE

The machining process is performed in ELECTRONICA EMS5030 machine; the work piece is mounted on the V-block which is located on the machine with magnetic table. The tool holder holds the tool and dial gauge has been used to test its alignment. The 54 runs were decided involving various parameter combinations based on Analysis of Variance. Portable roughness tester SJ201 has been utilized to measure roughness which is shown in Figure 3. The various input parameters level and the output are given in the Table 1 and 2.

Table 1: Different Variables Used in the Experiment and Their Levels

Variable	Coding	Level		
		1	2	3
Discharge Current (I_p) in A	A	10	65	70
Discharge Voltage in V	B	25	10	15
Pulse on Time (T_{on}) in μs	C	15	30	45
Pulse off Time (T_{off}) in s	D	1	7	9
Oil Pressure in kg/cm^2	E	20	0.2	0.3
Gap Width(mm)	F	0.04	0.22	0.4

Table 2: Planning matrix of the Experiments with the Optimal Model Data

Sl.No.	Input Parameters						Output Parameters			
	A	B	C	D	E	F	Experimental Output Through RSM		Predicted Output Through ANN	
	Current (A)	Voltage (V)	Pulse On Time (µs)	Pulse Off Time(Sec)	Oil Pressure (kg/cm ²)	Gap Width (mm)	G MRR (mg/sec)	H SR (µm)	MRR (mg/sec)	SR (µm)
1.	15	50	20	1.5	25	0.22	0.481	3.110	0.4615	2.9924
2.	15	50	20	2.0	25	0.22	0.470	3.163	0.3234	3.0709
3.	15	50	15	1.5	25	0.22	0.366	2.673	0.3610	2.6672
4.	15	75	20	1.5	25	0.22	0.459	2.950	0.4750	2.8839
5.	15	50	20	1.0	25	0.22	0.480	3.300	0.5415	3.4480
6.	15	25	20	1.5	25	0.22	0.390	2.371	0.2789	2.3033
7.	15	50	20	1.5	25	0.04	0.511	3.535	0.5152	3.5080
8.	25	50	20	1.5	25	0.22	0.531	3.490	0.3923	3.4670
9.	15	50	20	1.5	20	0.22	0.445	2.970	0.6533	3.0973
10.	15	50	25	1.5	25	0.22	0.411	2.750	0.3537	2.8122
11.	15	50	20	1.5	25	0.22	0.481	3.110	0.4615	2.9924
12.	15	50	20	1.5	25	0.40	0.461	3.468	0.4478	2.8721
13.	15	50	20	1.5	30	0.22	0.473	3.011	0.4088	2.9000
14.	5	50	20	1.5	25	0.22	0.379	2.391	0.2836	2.2736
15.	25	25	25	2.0	20	0.40	0.351	2.930	0.1173	2.5712
16.	5	25	15	2.0	30	0.04	0.133	0.870	0.1858	1.6289
17.	5	25	15	1.0	20	0.04	0.143	1.187	0.2204	1.4995
18.	15	50	20	1.5	25	0.22	0.481	3.110	0.4615	2.9924
19.	25	25	15	2.0	30	0.40	0.334	2.824	0.4290	2.9696
20.	25	75	15	1.0	20	0.04	0.331	2.986	0.5562	3.2147
21.	25	25	25	1.0	30	0.40	0.362	3.421	0.2019	1.6229
22.	5	75	15	2.0	30	0.40	0.230	2.640	0.1816	2.4910
23.	25	75	25	2.0	20	0.04	0.403	2.947	0.3714	2.9324
24.	5	75	15	1.0	20	0.40	0.242	2.379	0.5397	3.0684
25.	15	50	20	1.5	25	0.22	0.481	3.110	0.4615	2.9924
26.	5	75	25	2.0	20	0.40	0.267	2.410	0.2810	2.3269
27.	25	75	15	2.0	30	0.04	0.347	2.660	0.3194	2.7343
28.	5	75	25	1.0	30	0.40	0.307	2.682	0.4086	2.9642
29.	25	25	15	1.0	20	0.40	0.296	3.100	0.3987	3.0971
30.	5	25	25	2.0	20	0.04	0.198	1.040	0.2663	1.1700
31.	5	25	25	1.0	30	0.04	0.187	1.281	0.3585	1.3927
32.	25	75	25	1.0	30	0.04	0.410	2.648	0.3750	3.0516
33.	15	50	20	1.5	25	0.22	0.481	3.110	0.4615	2.9924
34.	15	50	20	1.5	25	0.22	0.481	3.110	0.4615	2.9924
35.	25	75	15	2.0	20	0.40	0.288	2.630	0.2999	2.6088
36.	25	25	25	2.0	30	0.04	0.428	2.960	0.1254	2.1964
37.	5	75	15	1.0	30	0.04	0.292	2.524	0.2732	2.5085
38.	25	25	25	1.0	20	0.04	0.389	3.413	0.4213	3.5370
39.	5	25	25	1.0	20	0.40	0.128	1.137	0.0738	0.7842
40.	5	75	15	2.0	20	0.04	0.257	2.660	0.2321	2.9370
41.	15	50	20	1.5	25	0.22	0.481	3.110	0.4615	2.9924
42.	25	75	15	1.0	30	0.40	0.355	2.816	0.3577	2.9326
43.	25	75	25	2.0	30	0.40	0.360	2.760	0.3322	2.5350
44.	15	50	20	1.5	25	0.22	0.481	3.110	0.4615	2.9924
45.	25	25	15	2.0	20	0.04	0.367	3.020	0.4939	2.0664
46.	25	25	15	1.0	30	0.04	0.362	3.076	0.0452	2.9142
47.	5	75	25	2.0	30	0.04	0.327	2.592	0.0809	2.8737
48.	5	75	25	1.0	20	0.04	0.330	2.560	0.2140	2.3010
49.	5	25	15	2.0	20	0.40	0.069	0.576	0.0028	0.5435
50.	15	50	20	1.5	25	0.22	0.481	3.110	0.4615	2.9924
51.	5	25	25	2.0	30	0.40	0.126	1.160	0.2268	2.7405
52.	25	75	25	1.0	20	0.40	0.350	2.730	0.6014	2.8535
53.	5	25	15	1.0	30	0.40	0.121	1.250	0.0749	1.0947
54.	15	50	20	1.5	25	0.22	0.481	3.110	0.4615	2.9924

IV. MODELING OF MRR AND SR

Based on the conditions of design matrix, the machining operations were performed at random to make error free measurement. In subsequent step, the plan in accomplishing the experiments implementing RSM utilizing a Box Behnken approach with six variables. Total count of experiments performed with the association of machining parameter are illustrated in Table 2. Models of MRR and SR are obtained by using Minitab software are equation 1 and 2. All the experimental values and the predicted input values are taken for the analysis for finding optimized inputs. Ultimate response equation for MRR and SR is shared as follows:

$$MRR = (-2.27473 + 0.01960A + 0.01238B + 0.15318C + 0.08097D + 0.04702E - 0.19114F - 0.00026A*A - 0.00009B*B - 0.00369C*C - 0.02323D*D - 0.00087E*E + 0.16025F*F - 0.00015A*B + 0.00104A*D + 0.00006 A*E + 0.00002 B*C - 0.00039 B*D + 0.00001B*E + 0.00085 B*F + 0.00142 C*D - 0.00011 C*E - 0.00431 C*F - 0.00128 D*E - 0.05278 D*F + 0.00472 E*F) \text{ Equation (1)}$$

$$SR = (-10.3534 + 0.2333A + 0.1146B + 0.6798C - 1.6742D + 0.2769E - 7.7338F - 0.0019 A*A - 0.0008 B*B - 0.0168 C*C + 0.4028 D*D - 0.0056 E*E + 11.4411 F*F - 0.0018 A*B - 0.0025 A*D - 0.0010 A*E - 0.0004 B*C + 0.0061 B*D - 0.0001 B*E + 0.0046 C*D + 0.0003 C*E + 0.0193C*F - 0.2288 D*F + 0.0994 E*F) \text{ Equation(2)}$$

Where →

- A - Working Current
- B - Working Voltage
- C -Pulse ON Time
- D -Pulse OFF Time
- E - Oil Pressure
- F - Spark Gap

V. ARTIFICIAL NEURAL NETWORKS ARCHITECTURE

Generally ANN consists of a number of layers: the layer where the input patterns are applied is called the input layer, the layer where the output is obtained is the output layer, and the layers between the input and output layers are the layers that are hidden are shown in Figure 4. One or more hidden layers are present, which are so named because their outputs are not directly observable. When the size of the input layer is large, the addition of hidden layers makes possible the network to extract higher-order statistics which are predominantly valuable. Fully or partially interconnected neurons layers are preceding and subsequent layer of neurons with each interconnection having an associated connection strength (or weight). In a forward direction, the input signal propagates through the network, on a layer-by-layer basis which is commonly referred to as Multilayer Perceptrons (MLP). Many publications discuss the development and theory of ANN.

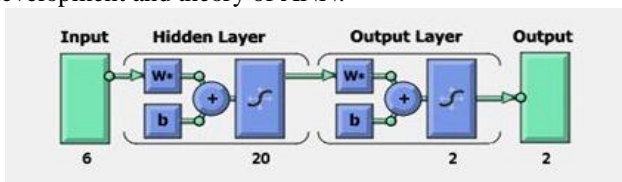


Figure 4: General Configuration of Artificial Neural Network

VI. BACK-PROPAGATION NETWORK ALGORITHM

The algorithm for the back-propagation network program is depicted below with the support of flow diagram as shown in Figure 5.

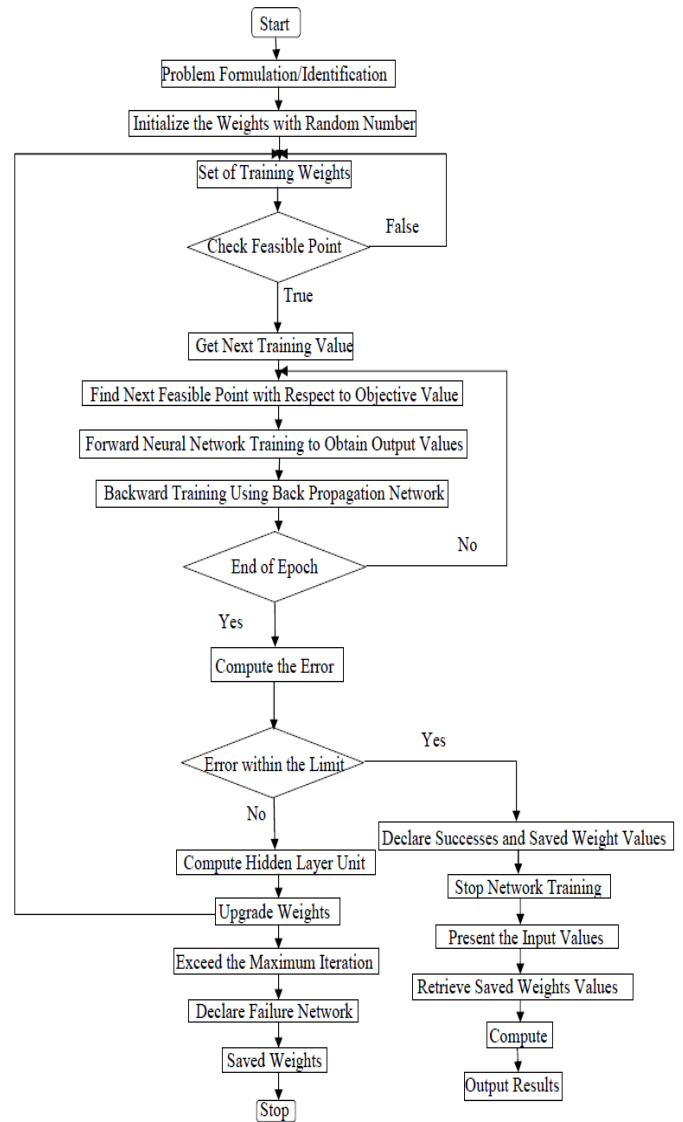


Figure 5: Back-Propagation Network Program

- Step 1:** Confirm the number of hidden layers.
- Step 2:** Confirm the neurons count for the input layer and the output layer. The neurons number equalizes the number of input variables for input layer and equalizes the number of outputs required for the output layer. Set few neurons count for the hidden layer.
- Step 3:** Get the input pattern of training.
- Step 4:** Assign neurons with small weight values interconnected between the input, hidden and output layers.
- Step 5:** Compute all the neurons output layers that are in hidden and output layers utilizing the succeeding formula.

$$Out_i = f \left(\sum_{w_{ij}} Out_j + q_1 \right) \text{ Equation (3)}$$

Where output_i is the output of the ith neuron in the layer under consideration; output_j is the output of the jth neuron in the preceding layer. f is the sigmoid function can be expressed as:

$$f(\text{net}_1) = \frac{1}{1 + e^{-\text{net}_i/q}} \quad \text{Equation (4)}$$

Where q is termed as temperature.

Step 6: Determine the output at the output layer and compare it with the desired output values. Determine the error of the output neurons,

$$\text{Error} = \text{desired output} - \text{actual output} \quad \text{Equation(5)}$$

Similarly, determine the root mean square error value of the output neurons.

Step 7: Determine the error existing at the hidden layers neurons and back-propagate those errors to the weight values associated between the neurons of input layer and hidden layer.

Likewise, back propagate the errors accessible at the output neurons to the weight values associated in between the hidden layer neurons and output layer utilizing the ensuing formula.

$$E_p = \frac{1}{2} \sum (t_{pj} - O_{pj})^2 \quad \text{Equation (6)}$$

Where E_p is the error for the pth presentation vector, t_{pj} is the desired value for the jth output neuron and O_{pj} is the desired output of the jth output neuron.

$$\text{error} \delta_{pi} = (t_{pi} - o_{pi}) o_{pi} (1 - o_{pi}) \quad \text{Equation (7)}$$

For output neurons,

$$\text{error} \delta_p = (t_{pi} - O_{pi}) O_{pi} \sum \delta_{pi} W_{ki} \quad \text{Equation (8)}$$

for hidden neurons Weight adjustment is made as follows:

$$\Delta W_{ji}(n = 1) = \eta(\delta_{pi} O_{pi}) = \alpha \Delta W_{ji}(n) \quad \text{Equation (9)}$$

Where η is the learning rate parameter and α is momentum factor.

Step 8: Go to Step 3 and perform the calculations up to Step 7 at the end of cycle regulate the root-mean-square error value, mean percentage of error and worst percentage of error above the complete patterns. For reaching Step 9 check for reasonable error, if so, go to Step 9 else go to Step 3 and reiterate the same from Step 3 to Step 7.

Step 9: Discontinue the iteration and the final weight values are noted that belongs to the neurons hidden layer and also to the output layer.

Step 10: Testing neural network model with the proficient weight values, regulate the output for the testing pattern and check whether the deviation from anticipated value is reasonably less or not.

If not, try the back propagation with reviewed network by modifying the number of neurons, varying learning rate parameters, momentum value and temperature values as well.

Table 2 illustrates the typical observation of network performance while testing the pattern.

VII. GREY RELATIONAL ANALYSIS

Grey Relational Analyses are implemented in determining the appropriate choice of machining parameters for Electrical Discharge Machining (EDM) process.

7.1. Steps IN GRA

Subsequent steps to be followed while implementing grey relational analysis for finding the Grey relational coefficients and the grey relational grade:

(a) Normalizing the experimental outcomes of MRR and surface roughness for avoiding the influence of adopting dissimilar units to decline the variability.

$$Z_j = \frac{y_{ij} - \min(y_{ij}, i=1,2,\dots,n)}{\max(y_{ij}, i=1,2,\dots,n) - \min(y_{ij}, i=1,2,\dots,n)} \quad \text{Equation (10)}$$

$$Z_j = \frac{\max(y_{ij}, i=1,2,\dots,n) - y_{ij}}{\max(y_{ij}, i=1,2,\dots,n) - \min(y_{ij}, i=1,2,\dots,n)} \quad \text{Equation (11)}$$

(b) Performing the grey relational generating and calculating the grey coefficient for the normalized values yield.

$$\gamma(y_0(k), y_j(k)) = \frac{\Delta_{\min} + \xi \Delta_{\max}}{\Delta_{oj}(k) + \xi \Delta_{\max}} \quad \text{Equation(12)}$$

Where,

- ✓ j=1, 2...n; k=1, 2...m, n is the number of experimental data items and m is the number of responses.
- ✓ y₀(k) is the reference sequence (y₀(k)=1, k=1, 2...m); y_j(k) is the specific comparison sequence.
- ✓ Δ_{oj} = ||y₀(k) - y_j(k)|| = The absolute value of the difference between y₀(k) and y_j(k).
- ✓ Δ_{min} = minmin ||y₀(k) - y_j(k)|| is the smallest value of y_j(k).
- ✓ Δ_{max} = maxmax ||y₀(k) - y_j(k)|| is the largest value of y_j(k).
- ✓ ζ is the distinguishing coefficient which is defined in the range 0 ≤ ζ ≤ 1 (the value may adjusted based on the practical needs of the system).

(c) Calculating the grey relational grade by averaging the grey relational coefficient yields:

$$\gamma_j = \frac{1}{k} \sum \gamma_{ij} \quad \text{Equation(13)}$$

Where γ_j is the grey relational grade for the jth experiment and the number of performance characteristics is k. Equation (10) is utilized in normalizing the experimental value when the default value target is having the characteristic of 'higher the better'.

Here MRR is normalized utilizing the above Equation (11). When the 'lower the better' is a characteristic of the default sequence, then it is normalized implementing Equation (12), i.e., surface roughness is normalized via this equation.

Using Equation (12), grey relational coefficient has been calculated for MRR and SR as illustrated in Table 2. Also the grey relational grade is figured as per Equation (13).



Table 2: Gray Relational Grade

Sl. No.	MRR	SR	Normalized Values for MRR	Normalized Values for SR	GRC Values for MRR	GRC Values for SR	Grade
1.	0.481	3.11	0.108225	0.14363	0.822064	0.776844	0.799454
2.	0.47	3.163	0.132035	0.125718	0.791096	0.799082	0.795089
3.	0.366	2.673	0.357143	0.291315	0.583333	0.63186	0.607597
4.	0.459	2.95	0.155844	0.197702	0.762376	0.716638	0.739507
5.	0.48	3.3	0.11039	0.079419	0.819149	0.862934	0.841041
6.	0.39	2.371	0.305195	0.393376	0.620968	0.559675	0.590321
7.	0.511	3.535	0.04329	0	0.920319	1	0.960159
8.	0.531	3.49	0	0.015208	1	0.970482	0.985241
9.	0.445	2.97	0.186147	0.190943	0.728707	0.723649	0.726178
10.	0.411	2.75	0.25974	0.265292	0.65812	0.653345	0.655732
11.	0.481	3.11	0.108225	0.14363	0.822064	0.776844	0.799454
12.	0.461	3.468	0.151515	0.022643	0.767442	0.956676	0.862059
13.	0.473	3.011	0.125541	0.177087	0.799308	0.738458	0.768883
14.	0.379	2.391	0.329004	0.386617	0.603133	0.563941	0.583537
15.	0.351	2.93	0.38961	0.204461	0.562044	0.709763	0.635903
16.	0.133	0.87	0.861472	0.900642	0.36725	0.356979	0.362114
17.	0.143	1.187	0.839827	0.793511	0.373183	0.386545	0.379864
18.	0.481	3.11	0.108225	0.14363	0.822064	0.776844	0.799454
19.	0.334	2.824	0.426407	0.240284	0.53972	0.675417	0.607568
20.	0.331	2.986	0.4329	0.185536	0.535963	0.729357	0.63266
21.	0.362	3.421	0.365801	0.038527	0.5775	0.928459	0.75298
22.	0.23	2.64	0.651515	0.302467	0.434211	0.623079	0.528645
23.	0.403	2.947	0.277056	0.198716	0.643454	0.715599	0.679526
24.	0.242	2.379	0.625541	0.390673	0.444231	0.561374	0.502802
25.	0.481	3.11	0.108225	0.14363	0.822064	0.776844	0.799454
26.	0.267	2.41	0.571429	0.380196	0.466667	0.568055	0.517361
27.	0.347	2.66	0.398268	0.295708	0.556627	0.628371	0.592499
28.	0.307	2.682	0.484848	0.288273	0.507692	0.634298	0.570995
29.	0.296	3.1	0.508658	0.147009	0.495708	0.772787	0.634247
30.	0.198	1.04	0.720779	0.84319	0.409574	0.372248	0.390911
31.	0.187	1.281	0.744589	0.761744	0.401739	0.396277	0.399008
32.	0.41	2.648	0.261905	0.299763	0.65625	0.625185	0.640717
33.	0.481	3.11	0.108225	0.14363	0.822064	0.776844	0.799454
34.	0.481	3.11	0.108225	0.14363	0.822064	0.776844	0.799454
35.	0.288	2.63	0.525974	0.305847	0.487342	0.620466	0.553904
36.	0.428	2.96	0.222944	0.194322	0.691617	0.720127	0.705872
37.	0.292	2.524	0.517316	0.341669	0.491489	0.594057	0.542773
38.	0.389	3.413	0.307359	0.04123	0.619303	0.923821	0.771562
39.	0.128	1.137	0.872294	0.810409	0.364353	0.38156	0.372957
40.	0.257	2.66	0.593074	0.295708	0.457426	0.628371	0.542898
41.	0.481	3.11	0.108225	0.14363	0.822064	0.776844	0.799454
42.	0.355	2.816	0.380952	0.242987	0.567568	0.672959	0.620263
43.	0.36	2.76	0.37013	0.261913	0.574627	0.656243	0.615435
44.	0.481	3.11	0.108225	0.14363	0.822064	0.776844	0.799454
45.	0.367	3.02	0.354978	0.174045	0.58481	0.74179	0.6633
46.	0.362	3.076	0.365801	0.15512	0.5775	0.763219	0.670359
47.	0.327	2.592	0.441558	0.318689	0.531034	0.610733	0.570884
48.	0.33	2.56	0.435065	0.329503	0.534722	0.60277	0.568746
49.	0.069	0.576	1	1	0.333333	0.333333	0.333333
50.	0.481	3.11	0.108225	0.14363	0.822064	0.776844	0.799454
51.	0.126	1.16	0.876623	0.802636	0.363208	0.383837	0.373522
52.	0.35	2.73	0.391775	0.272051	0.56068	0.647625	0.604152
53.	0.121	1.25	0.887446	0.77222	0.360374	0.393014	0.376694
54.	0.481	3.11	0.108225	0.14363	0.822064	0.776844	0.799454

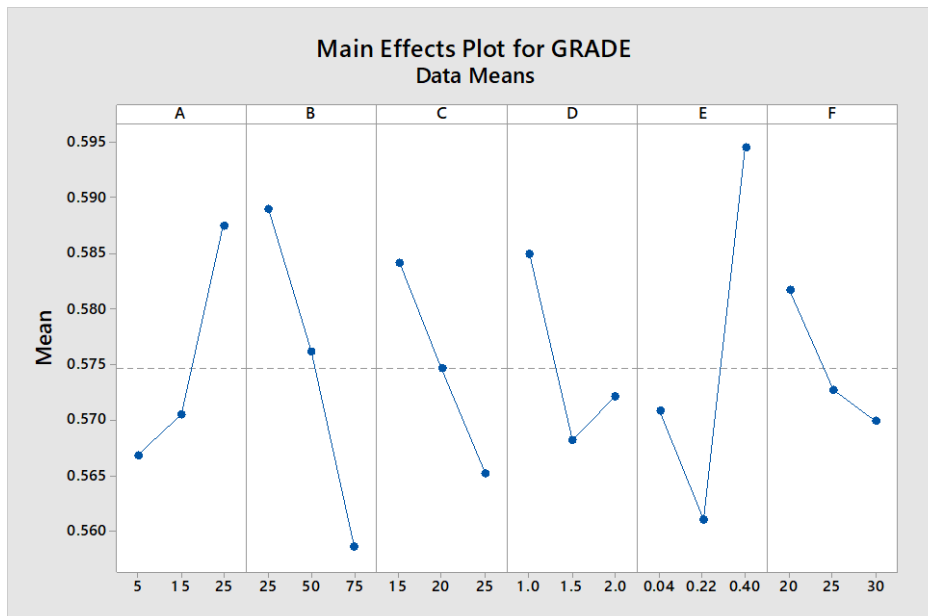


Figure 6: Main Effect Plot of Inpu

t Parameters for AISI1020 Steel

As observed in Table 3 MRR enhances from 0.362 Mg/sec to 0.404 Mg/sec and SR value was reduced from 3.421µm to 2.06 µm. Depending upon the specified results, it has been noticed that quality characteristics proves to be significantly enhanced via this confirmation test.

Table 3: Optimal Input and Output Parameters for AISI1020 Steel

Response	Process Parameters						Output	
	A (V) Voltage	B (A) Current	C (s) Pulse	D (s) Pulse	E (m) G	F Oil Pressure	MRR (Mg/sec)	SR (µm)
Initial	25	25	25	1.0	0.	30	0.36	3.4
Optimal	25	25	15	1	0.	20	0.40	2.0

VIII. RESULT AND DISCUSSION

8.1. Result and Discussion for MRR

Machining parameters effect (I_p , V, T_{on} , T_{off} , P_{oil} and spark gap) on the response variables MRR too were assessed by performing experiments. Outcomes are shared with the Minitab software for auxiliary analysis. Second-order model has been projected in finding the association between the MRR and the process variables brought into account. The analysis of variance (ANOVA) has been utilized in checking the sufficiency of the second order model.

Figure 7 illustrates the estimated response surface for MRR in association to the process parameters of pulse current and pulse on time which could be viewed from the figure, the MRR have a tendency to rise up, considerably with rise in peak current for any value of pulse on time. Henceforward, maximum MRR is achieved at high peak current and high pulse on time which is because of their dominant control over the input energy i.e. with the rise in pulse current produces strong spark that produces greater temperature ending up in melting of more material and the work piece erosion.

The effect of I_p and T_{off} is on the estimated response surface of MRR is illustrated in the Figure 8, the parameters

T_{on} , V, spark gap and P_{oil} stays unchanged in its maximum level. MRR rises up when I_p goes up, the explanation is similar, as mentioned earlier, though with the rise in T_{off} , MRR declines, which is because when T_{off} increases, there exist an uninvited heat loss that does not subsidize to MRR leading to the work piece temperature drop before the next spark begins and hence MRR declines. The maximum MRR is attained with high I_p and lower T_{off} for the provided choice of input parameters. Figure 9 illustrates MRR as a function of T_{on} and T_{off} , while the I_p , V, spark gap and P_{oil} remains constant in its higher level that could be viewed that the highest MRR values occurred at the higher T_{on} and at the lower T_{off} . Figure 10 represents MRR as a function of V and I_p , whereas the T_{on} , T_{off} , spark gap and P_{oil} remains constant in its higher level. It can be seen that the highest MRR values took place at the higher I_p and V.

Figure 11 represents MRR as a utility of T_{on} and current, while the I_p , voltage, T_{off} , spark gap and P_{oil} remains constant in its higher level with the highest MRR values occurred at higher T_{on} and current. Figure 12 represents MRR as a function of Current and T_{off} , while the I_p , T_{on} , voltage, spark gap and P_{oil} remains constant in its higher level with higher MRR values occurred at the higher current and lower T_{off} . Figure 13 represents MRR as a function of P_{oil} and voltage, whereas the T_{on} , spark gap, T_{off} and current remains constant in its higher level. It can be seen that the highest MRR values occurred at the higher voltage and medium P_{oil} .

Figure 14 represents MRR as a function of T_{off} and P_{oil} , while the I_p , spark gap, T_{on} and V remains constant in its higher level with the highest MRR values occurring at the lower T_{off} and of P_{oil} . Figure 15 represents MRR as a function of spark gap and voltage, whereas the I_p , T_{off} , T_{on} and current remains constant in its higher level. It can be seen that the highest MRR values occurred at the lower spark gap and higher voltage.

Figure 16 represents MRR as a function of spark gap and voltage, whereas the I_p, T_{off}, T_{on} and V remains constant in its higher level. It can be seen that the highest MRR values occurred at the lower spark gap and higher voltage. Figure 17 represents MRR as a function of spark gap and current, while the voltage, T_{off}, T_{on} and P_{oil} remains constant in its higher level with high MRR values occurred at the lower spark gap and higher current. Figure 18 represents MRR as a function of spark gap and p_{off} , while the I_p, T_{on}, p_{oil} and V remains constant in its higher level with highest MRR

values occurred at the lower spark gap and lower pulse off time. Figure 19 for MRR is shown in along with the various parameters using RSM and ANN. ANN is an appropriate tool, used in calculating the material removal rate in machining process. Outcomes illustrate that ANN model has been efficaciously functional to the machining parameters of AISI 1020 Steel. It is observed from Figure 19(Validation of RSM and ANN model for MRR) that predicted depending upon ANN model is very close to the experimental surveillance.

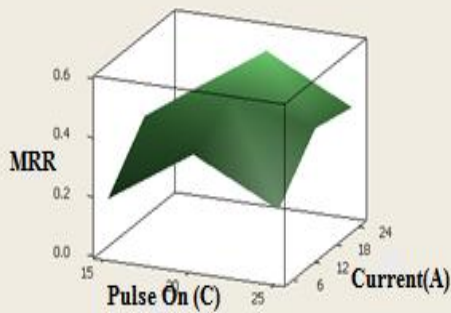


Figure 7: MRR Vs Pulse On Time and Current

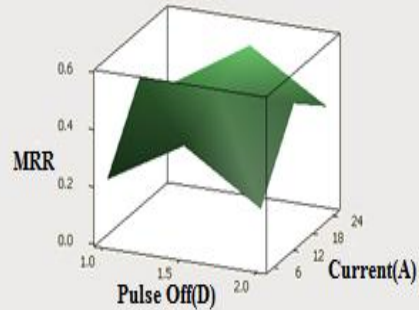


Figure 8: MRR Vs Pulse Off Time and Current

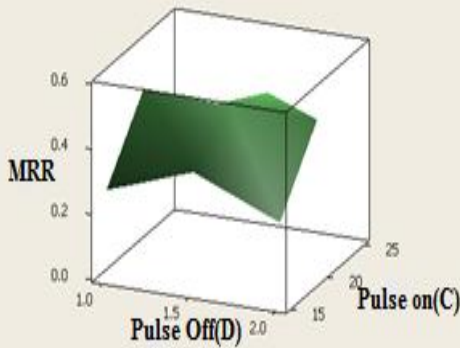


Figure 9: MRR Vs Pulse Off Time and Pulse on Time

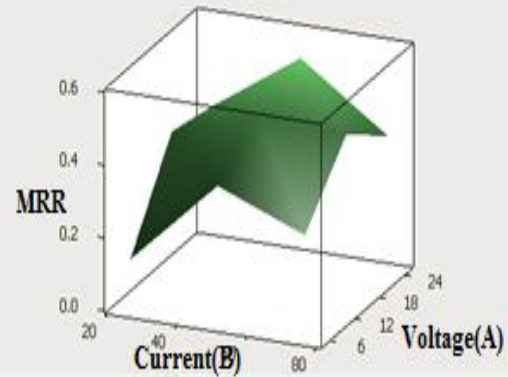


Figure 10: MRR Vs Current and Voltage

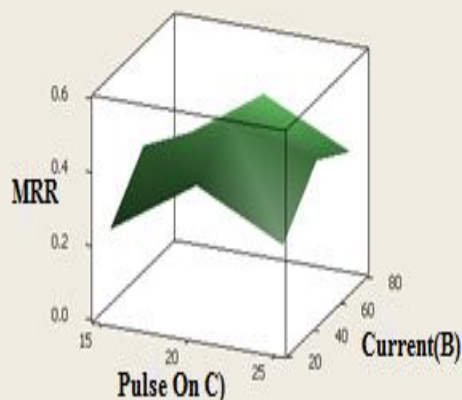


Figure 11: MRR Vs Pulse on Time and Current

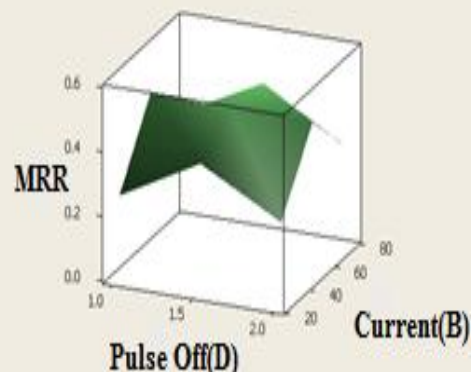


Figure 12: MRR Vs Pulse Off Time and Current

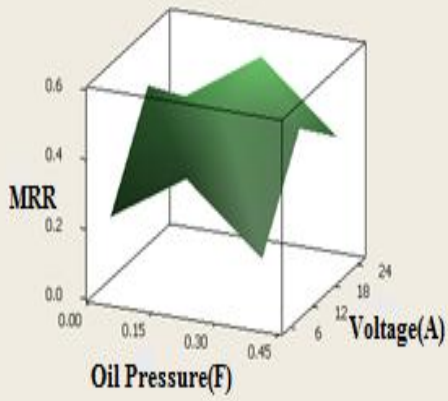


Figure 13: MRR Vs Oil Pressure and Voltage

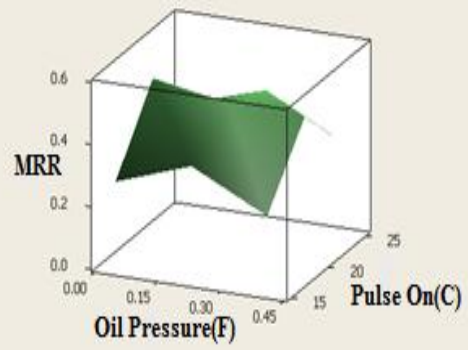


Figure 14: MRR Vs Oil Pressure and Pulse On Time

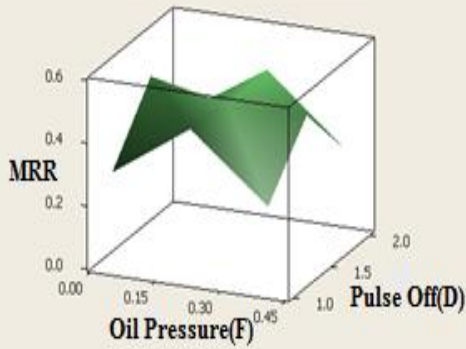


Figure 15: MRR Vs Oil Pressure and Pulse OFF Time

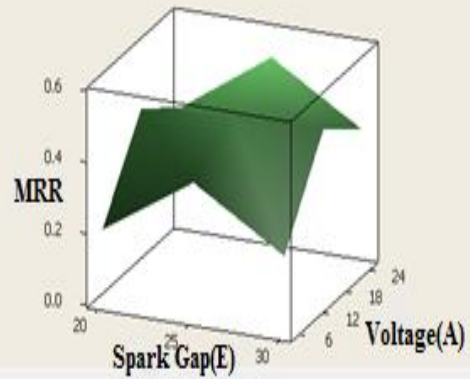


Figure 16: MRR Vs Spark Gap and Voltage

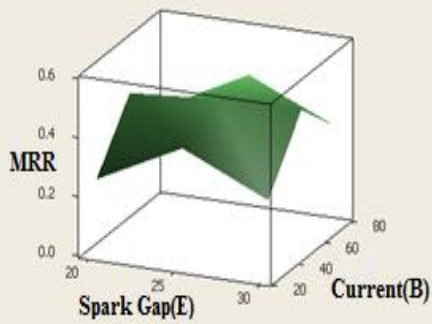


Figure 17: MRR Vs Spark Gap and Current

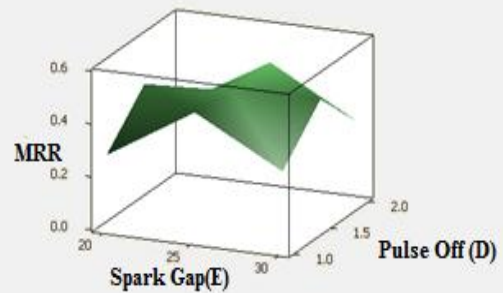


Figure 18: MRR Vs Spark Gap and Pulse Off Time

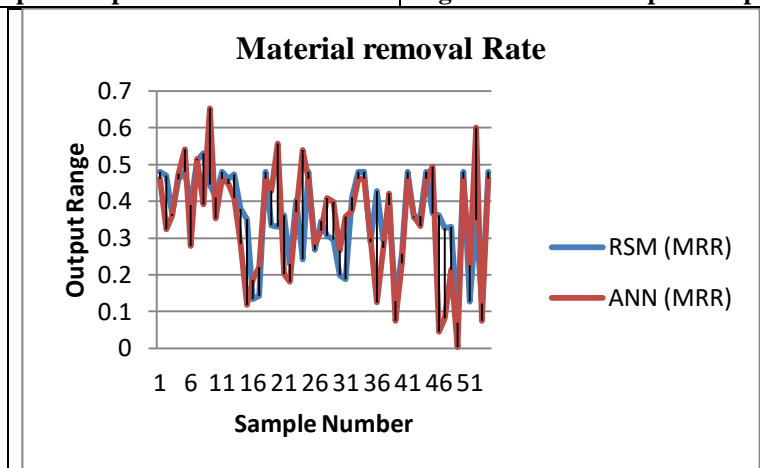


Figure 19: Variation of MRR for RSM and ANN

8.2. Result and Discussion for SR

Machining parameters effect (I_p, V, T_{on}, T_{off} , spark gap and P_{oil}) on the response variables SR was assessed by accompanying experiments. Outcomes are put into the Minitab software for additional analysis. The second-order model has been proposed for finding the association among the MRR and the process variables taken into account. The Analysis of Variance (ANOVA) has been utilized in checking the adequacy of the second order model. Figure 20 represents SR as a function of T_{off} and current, while the V, T_{on} , spark gap and P_{oil} remains constant at its lower levels with low range of SR values when T_{off} and V are greater. Figure 21 depicts SR as a function of current and T_{on} , while the V, T_{off} , spark gap and P_{oil} remains constant at its lower levels with SR values are high when current is low with higher T_{off} . Figure 22 represents SR as a function of T_{on} and T_{off} , whereas the I_p , spark gap, V and P_{oil} remains constant at its lower levels. It is observed that the SR values are low when T_{on} is low with higher T_{off} . Even though two parameter influences is very less on comparison with the effect of I_p on SR.

Figure 23 illustrates the estimated response surface for SR in association to the process parameters of I_p and T_{on} while T_{off}, V , spark gap and P_{oil} remain constant at their lowest values. Figure illustrates that the SR increases predominantly with the increase in I_p for any value of T_{on} . Though, the SR tends to rise up with rise in T_{on} , particularly at higher I_p .

Henceforward, minimum SR is achieved at low peak current and low pulse on time.

Which is due to their dominant control over the input energy, i.e. with the rise in I_p generating strong spark creating the higher temperature and crater, hence rough surface in the work piece and low I_p creates small crater and consequently smooth surface.

The effect of I_p and T_{off} is on the estimated response surface of SR is illustrated in Figure 24 T_{on}, V , spark gap and P_{oil} remains constant in its lower levels which could be noted that the SR goes up when the I_p, T_{off} goes up.

Figure 25 represents SR as a function of V and I_p , while the T_{on} , spark gap, T_{off} and P_{oil} remains constant at its lower levels with the observation that low range of SR values when V and I_p are low. Figure 26 illustrates SR as a function of oil pressure and I_p , while the T_{on} , voltage, T_{off} and spark gap remains constant at its lower levels with the observation that low range of SR values when oil pressure and I_p are low.

Oil pressure effect and T_{on} is on the estimated response surface of SR is portrayed in Figure 27. T_{off} , current, voltage and spark gap remains constant in its lower levels with the observation that rise in SR takes place when the oil pressure increases and pulse on time decreases. Figure 28 represents SR as a function of oil pressure and voltage, whereas the T_{on} , current, T_{off} and spark gap remains constant at its lower levels with the observation that the SR values are low when oil pressure and voltage are low.

Figure 29 illustrates SR as a function of V and spark gap, while the current, T_{on}, T_{off} and P_{oil} remains constant at its lower levels with the observation that the SR values are low when V and spark gap are high.

Figure 30 for SR is shown in along with the various parameters using RSM and ANN. ANN is an appropriate tool, used in calculating the surface roughness in machining process. ANN model has been tested and graph was plotted using determined and tested values.

The results illustrate that ANN model was implemented fruitfully to the machining parameters of AISI 1020 Steel. It is observed from Figure 30 (Validation of RSM and ANN model for SR) that predicted based on ANN model is highly adjacent to the observation of the experiment.

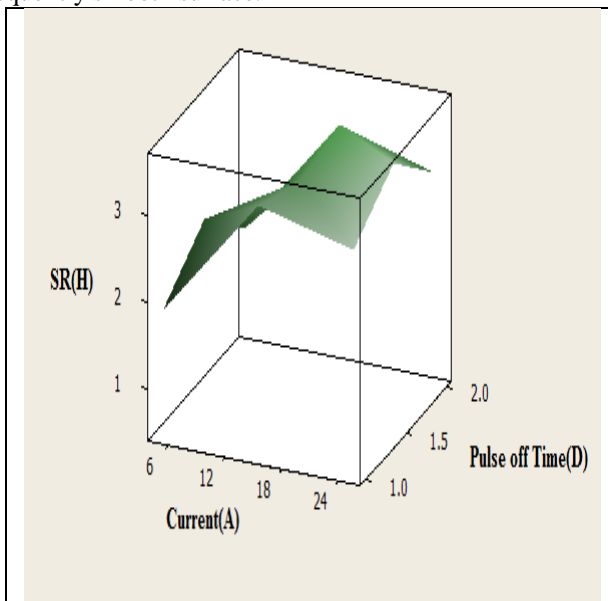


Figure 20: SR Vs Current and Pulse off Time

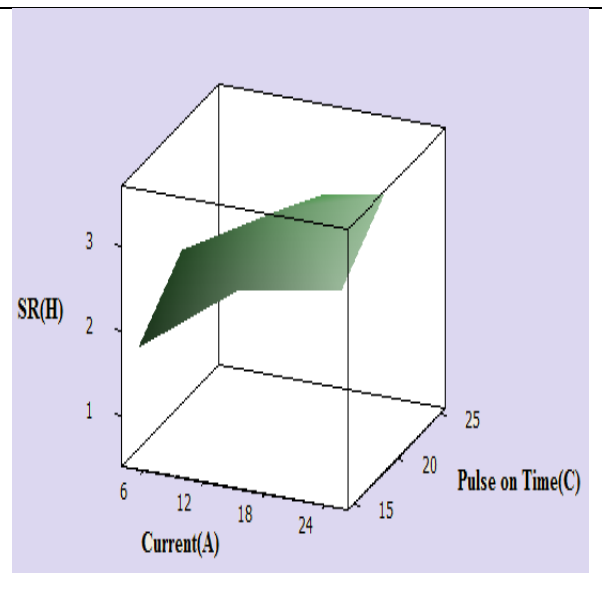


Figure 21: SR Vs Current and Pulse on Time

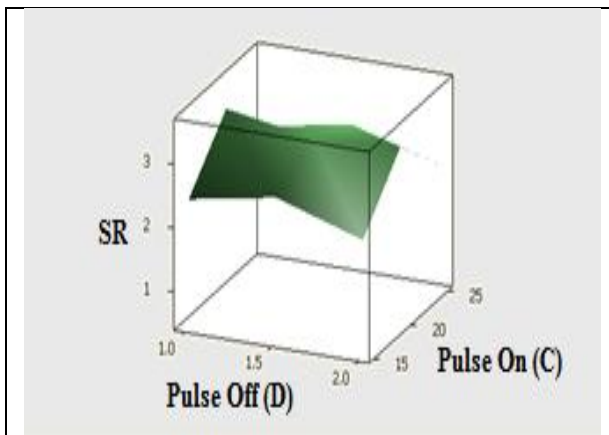


Figure 22: SR Vs Pulse off Time and Pulse on Time

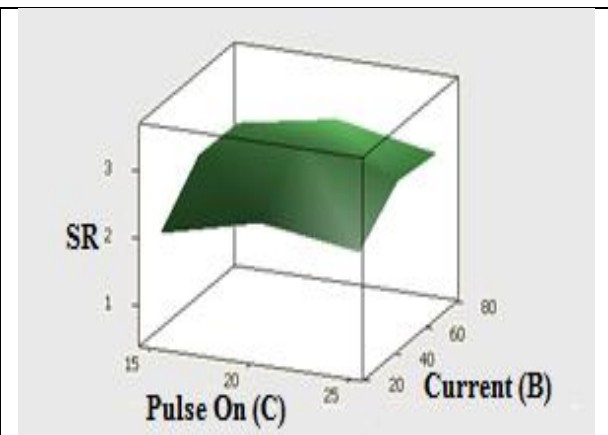


Figure 23: SR Vs Pulse on Time and Current

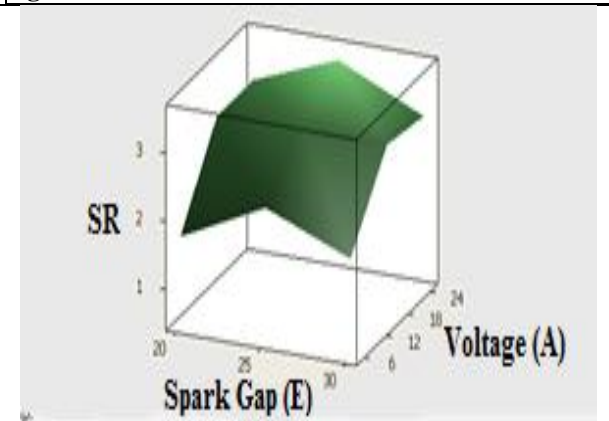


Figure 24: SR Vs Spark Gap and Voltage

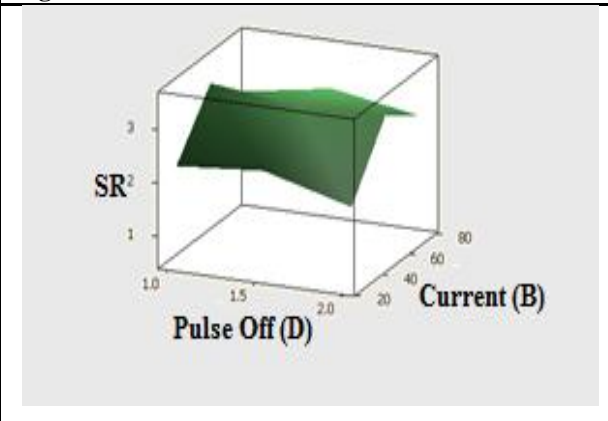


Figure 25: SR Vs Pulse off Time and Current

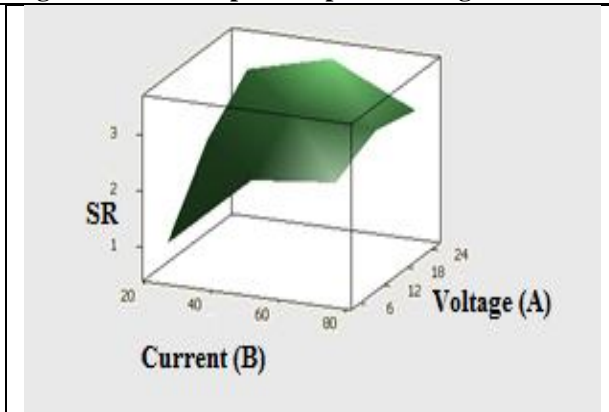


Figure 26: SR Vs Current and Voltage

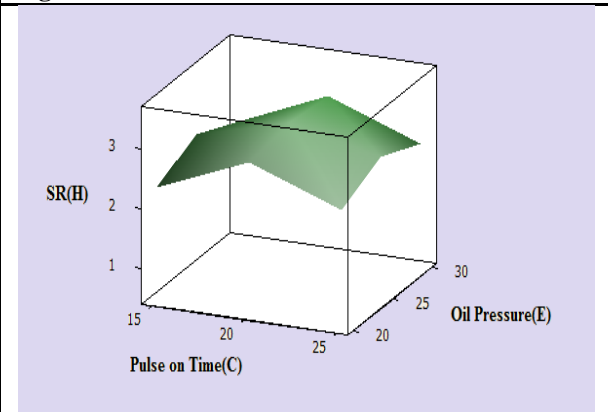


Figure 27: SR Vs Pulse on Time and Oil Pressure

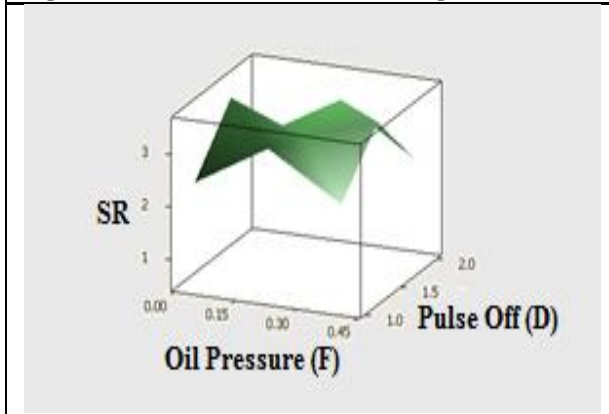


Figure 28: SR Vs Oil Pressure and Pulse off Time

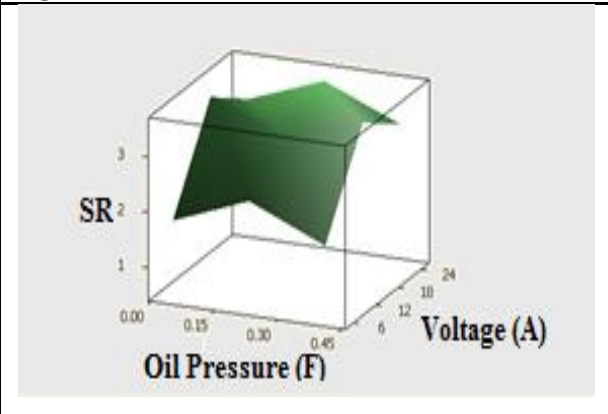


Figure 29: SR Vs Oil Pressure and Voltage

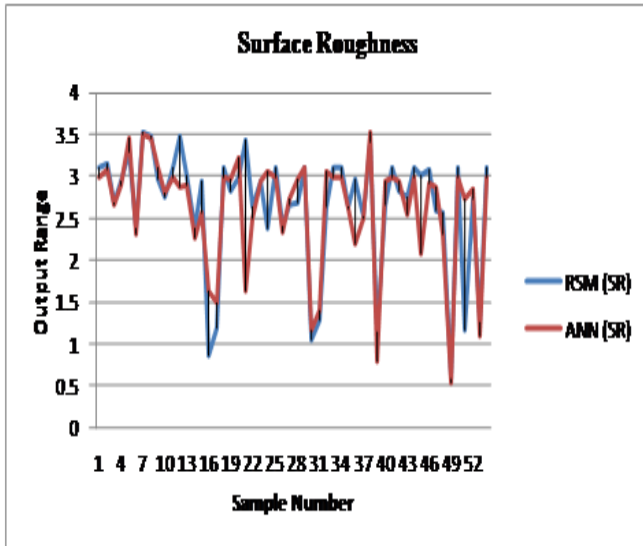


Figure 30: Variation of SR for RSM and ANN

IX. CONCLUSION

In this work, the input parameters are Discharge Current, Discharge Voltage, Pulse ON time, Pulse Off Time, gap width, Oil Pressure and Metal Removal Rate, Surface Roughness are the output machining parameters. Various levels of input conditions are consequential of RSM using Box Bekhen method. The experiments are performed on EDM machine, using the experimental results, two models viz., the RSM and ANN are created and calculated. GRA implemented to for finding the range of parameter influences in MRR and SR. The final conclusions based on these two prediction models, the ANN method with a kind of empirical model gives good result when compared with RSM model in terms of acceptable error.

REFERENCES

1. KuldeepOjha, Garg, R. K., Singh, K. K. (2010).MRR Improvement in Sinking Electrical Discharge Machining. A Review Journal Mining and Material Characterization and Engineering, Volume 9, Issue (8), pp. 709-739.
2. Krishna Mohana Rao. Gand Hanumantha Rao. D, (2010), Hybrid Modeling and Optimization of Hardness of Surface Produced by Electric Discharge Machining Using Artificial Neural Networks and Genetic Algorithm, International Journal of Engineering and Applied Science, Volume 5, Issue5, pp. 1819-6608.
3. Musrrat Ali, Millie Pant, and Singh. V. P. (2009). An Improved Differential Evolution Algorithm for Real Parameter Optimization Problems, International Journal of Recent Trends in Engineering, Volume1, Issue5, pp. 63-65.
4. Mahapatra.S and Amar Patnaik,(2006),Parametric Optimization of Wire Electrical Discharge Machining Process Using Taguchi Method, International Journal of Brazilian Society Mech. Science and Engineering, Volume28, Issue4, pp. 422-429.
5. Majumder, Arindam,(2012),Parametric Optimization of Electric Discharge Machining by GA-Based Response Surface Methodology, International Journal of Manufacturing Science and Production, Volume 12, pp. 25-30.
6. Puertas. I, Luisa. C. J, (2003), Study on the Machining Parameters Optimization of EDM, International Journal

- of Materials Processing and Technology, Volume 143-144, pp. 521-526
7. Qing Gao, Qin-He Zhang, Shu-peng SU, Jian-hua Zhang. (2008). Parameter Optimization Model in Electrical Discharge Machining Process, Journal of Zhejiang University Science. A9, 1, 104-108.
8. Ramezan Ali Mahdavi Nejad, (2011), Modeling and Optimization of EDM of SiC Parameters, Using Neural Network and Non-Dominating Sorting Genetic Algorithm (NSGA II), International Journal of Material Science and Applications, Volume2, pp. 669-675.
9. Shabgard M. R, Shotorbani. R. M, (2009), Mathematical Modeling of Machining Parameters in Electrical Discharge Machining of FW4 Welded Steel, World Academy of Science, International Journal of Engineering and Technology, Volume 3, pp. 04-29.
10. SushantDhar, Rajesh Purohit, NishantSaini, Akhil Sharma, HemathKumarb. G,(2007), Mathematical Modeling of Electric Discharge Machining of Cast Al-4Cu-6Si Alloy-10 wt.% SiC_p Composites, Journal Material Processing and Technology, Issue194, pp.24-29.
11. Sameh S. Habib, (2009), Study of the Parameters in EDM Through Response Surface Methodology Approach, Applied Mathematical Modelling, Volume 33, pp. 4397-4407.
12. Seung-Han Yanga, Srinivas. J, SekarMohana, Dong-MokLeea, Sree Balaji, B., (2009), Optimization of Electric Discharge Machining Using Simulated Annealing, Journal Material Processing and Technology, 2099, pp. 4471-4475.
13. Tolga Bozdana. A, Oguzhan Yilmaz, Ali Okka. M, Huseyin Filiz. I, (2010), Mathematical Modelling of EDM Hole Drilling Using Response Surface Methodology, Department of Mechanical Engineering, The University of Gaziantep, Volume 27310, pp. 90 - 94.
14. Thillaivanan. A, Asokan. P, Srinivasan. K. N. and Saravanan. R,(2010), Optimization of Operating Parameters for EDM Process Based on the Taguchi Method and Artificial Neural Network, International Journal of Engineering. Science and Technology, Volume 12, pp. 6880-6888.
15. Yan. B. H, Huang. F. Y, Chow. H. M, Tsai. J. Y., (1999), Micro-Hole Machining of Carbide by Electric Discharge Machining, Journal Material Processing and Technology, Volume 87, pp. 139-145.